Accepted Manuscript

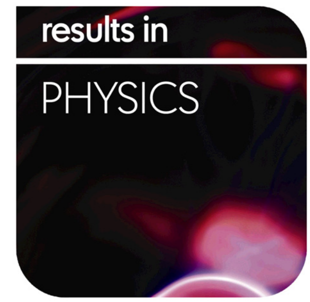

Magnetohydrodynamic dissipative flow across the slendering stretching sheet with temperature dependent variable viscosity

M. Jayachandra Babu, N. Sandeep, M.E. Ali, Abdullah. O. Nuhait

PII: S2211-3797(17)30574-0
DOI: http://dx.doi.org/10.1016/j.rinp.2017.05.018
Reference: RINP 703

To appear in: *Results in Physics*

Received Date: 5 April 2017
Revised Date: 21 May 2017
Accepted Date: 21 May 2017

Please cite this article as: Jayachandra Babu, M., Sandeep, N., Ali, M.E., Nuhait, h.O., Magnetohydrodynamic dissipative flow across the slendering stretching sheet with temperature dependent variable viscosity, *Results in Physics* (2017), doi: http://dx.doi.org/10.1016/j.rinp.2017.05.018

Magnetohydrodynamic dissipative flow across the slendering stretching sheet with temperature dependent variable viscosity

M. Jayachandra Babu[1] N. Sandeep[2*] M. E. Ali[3*] Abdullah O. Nuhait[4]

[1,2]Department of Mathematics, VIT University, Vellore-632014, India.
[3,4] Mechanical Engineering Department, College of Engineering, King Saud University, P. O. Box 800, Riyadh 11421, Saudi Arabia.
[2]Email: dr.nsrh@gmail.com [3]Email: mali@ksu.edu.sa

Abstract

The boundary layer flow across a slendering stretching sheet has gotten awesome consideration due to its inexhaustible pragmatic applications in nuclear reactor technology, acoustical components, chemical and manufacturing procedures, for example, polymer extrusion, and machine design. By keeping this in view, we analyzed the two-dimensional MHD flow across a slendering stretching sheet within the sight of variable viscosity and viscous dissipation. The sheet is thought to be convectively warmed. Convective boundary conditions through heat and mass are employed. Similarity transformations used to change over the administering nonlinear partial differential equations as a group of nonlinear ordinary differential equations. Runge-Kutta based shooting technique is utilized to solve the converted equations. Numerical estimations of the physical parameters involved in the problem are calculated for the friction factor, local Nusselt and Sherwood numbers. Viscosity variation parameter and chemical reaction parameter shows the opposite impact to each other on the concentration profile. Heat and mass transfer Biot numbers are helpful to enhance the temperature and concentration respectively.

Keywords: MHD; variable viscosity; viscous dissipation; convective boundary conditions; slendering stretching sheet.

Nomenclature:

A : non-dimensional variable viscosity parameter

u, v : velocity components in x, y directions $\left(ms^{-1}\right)$

f : dimensionless velocity of the fluid

N : coefficient related to stretching sheet

n : velocity power index parameter

c : physical parameter related to stretching sheet

$B(x)$: magnetic field parameter

T : temperature of the fluid $\left(K\right)$

k : thermal conductivity $\left(W\ m^{-1}\ K\right)$

k_0 : chemical reaction parameter

U_w : stretching velocity of the sheet $\left(ms^{-1}\right)$

C : concentration of the fluid $\left(kg\ \mathrm{m}^{-2}\right)$

C_p : specific heat at constant pressure $\left(\mathrm{J\ kg}\ K^{-1}\right)$

T_∞ : temperature of the fluid in the free stream $\left(K\right)$

C_∞ : concentration of the fluid in the free stream $\left(kg\ \mathrm{m}^{-2}\right)$

$\Pr$: Prandtl number

B_0 : magnetic field strength

$B(x)$: dimensional magnetic field parameter

M : magnetic field parameter

Sc : Schmidt number

Kr : dimensionless chemical reaction parameter

h_1 : heat transfer coefficient

h_2 : concentration transfer coefficient

a_1, b_1 : constants

Ec : Eckert number

C_f : skin friction coefficient

Nu_x : local Nusselt number

Sh_x : local Sherwood number

Re_x : local Reynolds number

Greek Symbols

ϕ : dimensionless concentration

ζ : similarity variable

σ : electrical conductivity of the fluid $\left(m\ \Omega\ m^{-1}\right)$

θ : dimensionless temperature

ρ : density of the fluid $\left(kg\ \mathrm{m}^{-3}\right)$

λ : wall thickness parameter

μ : dimensional variable viscosity parameter

μ^* : constant value of the coefficient of viscosity far away from sheet

υ : kinematic viscosity $\left(m^2\ \mathrm{s}^{-1}\right)$

β_1 : heat transfer Biot number

β_2 : mass transfer Biot number

1. Introduction

Several researchers have presumed that the properties of the fluid are changeless. Yet, tests recommended, this can be held just if the temperature does not change rapidly or quickly in a particular way. For lubing up fluids, warming created by the inside erosion and the comparing climb in temperature impacts the thickness of the liquid. In this manner, the fluid viscosity can never again be expected changeless. Sheet with variable thickness can be experienced all the more frequent in true applications. Plates with variable thickness are regularly utilized as a part of machine design, engineering, maritime structures, nuclear reactor technology and acoustical segments. The boundary layer flow across a slendering stretching sheet has gotten awesome consideration due to its inexhaustible pragmatic applications in nuclear reactor technology, acoustical components, chemical and manufacturing procedures, for example, polymer extrusion, and machine design. Elbashbeshy [1] and Hossain et al. [2] analyzed the impact of variable viscosity on the free convective fluid flow over a vertical plate within the sight of several parameters including magnetic field and radiation. They witnessed that (a) the local Nusselt number is substantially affected by the viscosity variation parameter (b) the magnetic field lessens the friction factor. Seddeek [3] modeled the unsteady MHD flow across a quasi-infinite flat plate by viewing aligned magnetic field along with the variable viscosity. He acknowledged that the viscosity parameter expands the temperature. By considering stretching sheet and variable viscosity, Abel et al. [4] and Mukhopadhyay et al. [5] studied the different fluid flows and analyzed the characteristics of heat transfer. They observed that (a) the permeability parameter lessens the skin friction parameter (b) variable viscosity of the fluid brings a substantial use in dislodging the fluid aside from the wall. Hassanien et al. [6] used finite difference scheme to discuss the impact of variable viscosity on the innate convection flow across an isothermal vertical wedge and cone. They reported that the viscosity variation parameter improves the heat transfer rate. By considering the similar impact alongside some different parameters including thermal stratification, Ali [7], Pantokratoras [8] and Afify [9] analyzed different flows such as non-Darcy MHD, Falkner-Skan. They saw that (a) the temperature dependent viscosity increases the shear stress for the small values of the buoyancy parameter (b) thermal stratification parameter lessens the Nusselt number (c) the viscosity parameter raises the wall heat transfer. Seddeek et al. [10] modelled the Hiemenz flow with several parameters including variable viscosity and also explained the features of the heat and mass transfer. Within the sight of thermal radiation and variable viscosity, Makinde and Ogulu [11] clarified the conduct of heat and mass transfer in the free convective flow across a vertical permeable plate. They discovered that the magnetic field parameter and the variable viscosity parameter displayed the opposite behavior on the wall shear stress.

The impact of the variable viscosity parameter and the viscoelastic parameter on the MHD flow across a stretching sheet are researched by Prasad et al. [12]. The interesting outcome of the work of Makinde [13] on the characteristics of entropy generation for the MHD flow with the viscous variation effect, is the friction factor is substantially improved by the viscosity variation parameter. Several authors [14-16] continued the work to analyze the influence of viscous variation parameter together with some different parameters on nanofluid flow across different channels. Few of their observations are (a) the viscosity parameter expands the denseness of the thermal boundary layer (b) the Cu-water nanofluid flow runs quicker when contrasted with Al_2O_3-water nanofluid (c) the impacts of the viscosity parameter and the magnetic field parameter on the velocity are indistinguishable.

Biot number is an amount of heat transferred to a body of a surface by means of convection and, it is circulated through the body through conduction which is subjected to the body's ability to store the thermal energy. Convective heat transfer studies have gotten significant consideration attributable to its imperative in procedures, including high temperatures, for example, nuclear plants, gas turbines, and thermal energy storage. Makinde and Aziz [17] numerically examined the impact of the convective boundary condition on MHD mixed convective flow across a vertical plate immersed in a permeable medium. They found that the Biot number rises both the velocity and temperature. After that, they [18] dissected the boundary layer flow of nanofluid with a similar supposition (convective boundary condition) across the stretching surface and, noticed that the denseness of the concentration layer increments with the rise in the Biot number. With the assumption of convective boundary conditions, Hayat et al. [19] and Alsaedi et al. [20] described the various fluids flows towards a stagnation point across the stretching surface. By considering the same conditions, Noghrehabadi et al. [21] theoretically investigated the characteristics of nanofluid flow across the stretching sheet within the sight of partial slip. They observed that the Nusselt and Sherwood numbers are enormously influenced by the Biot number and the slip factor.

Qasim [22] and Nadeem et al. [23] modeled the Blasius flow of Eyring-Powell fluid and a Casson fluid flow towards a stagnation point respectively, by viewing the similar boundary conditions along with some parameters including Soret and Dufour. Some of their findings are (a) Eyring-Powell fluid parameter lessens the denseness of the momentum boundary layer (b) Biot number prompts the decrease in local mass flux. Rahman et al. [24] used Buongiorno's model to explain the heat and mass transfer characteristics of a nanofluid under the same conditions. In the sight of slip and convective boundary conditions, Ibanez [25] analyzed MHD flow across a porous channel. He examined the effect of a few parameters, for example, Hartmann number and the Biot number on the global entropy generation. He reported that the Biot and Eckert numbers remain changeless on the impact of slip flow. With the assumption of same boundary conditions, Kandasamy et al. [26] and Waqas et al. [27] reported the mixed convection flow of different fluids (nano fluid and micropolar fluid) across different channels in the sight of various parameters including Soret number. Later, Naganthran and Nazar [28] made the stability analysis and numerical analysis of the nanofluid flow towards the stagnation-point across a stretching/shrinking sheet under the similar boundary conditions. They watched that the dual solutions existed for both cases and stability analysis demonstrated that the first solution is steady and physically feasible and the second solution is insecure. One of the discoveries of the Fang et al. [29] work on the momentum boundary layers across a slendering stretching sheet is the non-evenness of the sheet prompts to a mass suction and injection impacts for the velocity power index values less than one and greater than one respectively. Khader and Megahed [30] used the Chebshev spectral method in solving the problem of boundary layer flow across a stretching sheet with the variable thickness in the sight of slip effects. They discovered that the slip velocity lessens the friction factor. Anjali Devi and Prakash [31, 32] contributed some phenomenal work across the same channel (slendering stretching sheet). Few of their findings are (a) velocity slip parameter raise the temperature (b) viscosity and thermal conductivity parameters show the opposite behavior on the skin friction. Later this work was extended by Jayachandra Babu and Sandeep [33, 34] within the sight of different parameters, for example, thermophoresis and Brownian motion. Very recently, the researchers [35-40] investigated the heat transfer nature of various fluids by considering the different flow geometries.

So far no endeavor has been attempted towards the MHD flow across the slendering stretching sheet with convective boundary conditions within the sight of variable viscosity and viscous dissipation. We used Runge-Kutta based shooting technique to solve the converted equations. The impact of relevant parameters on the three regular profiles (velocity, temperature, and concentration) are displayed through the graphs and examined in details. And also, with the aid of the table, we have discussed the friction factor, local Nusselt and Sherwood numbers.

2. Mathematical Formulation

We have considered a steady, laminar, two-dimensional MHD flow of electrically conducting fluid across a slendering stretching sheet. We assumed the convective boundary conditions within the sight of variable viscosity and viscous dissipation parameters. Here our presumptions are $U_w(x) = b(x+c)^n$ and $y = N(x+c)^{\frac{1-n}{2}}$. We expect the magnetic Reynolds number as low as conceivable to disregard the induced magnetic field. In this work, $n \neq 1$ demonstrating that the sheet is having a variable thickness. The transverse magnetic field is applied as depicted in Fig.1. Induced magnetic field is neglected in this study.

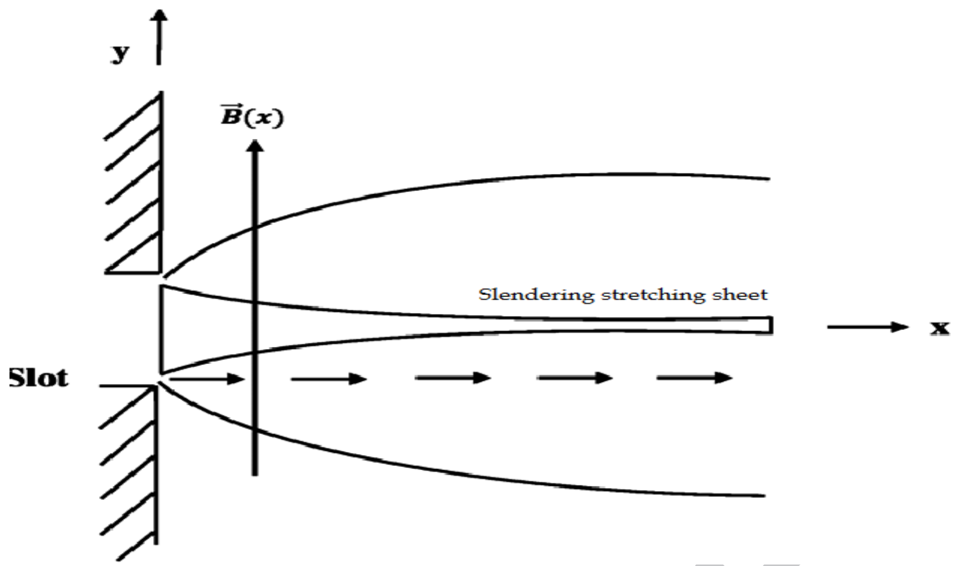

Fig.1 Physical model

Based on the above assumptions, the governing equations are

$$\frac{\partial u}{\partial x}+\frac{\partial v}{\partial y}=0, \tag{1}$$

$$\rho\left(u\frac{\partial u}{\partial x}+v\frac{\partial u}{\partial y}\right)=\frac{\partial}{\partial y}\left(\mu\frac{\partial u}{\partial y}\right)-\sigma B^2(x)u, \tag{2}$$

$$u\frac{\partial T}{\partial x}+v\frac{\partial T}{\partial y}=\frac{k}{\rho C_p}\frac{\partial^2 T}{\partial y^2}+\frac{\mu}{\rho c_p}\left(T_\infty\left(\frac{\partial u}{\partial y}\right)^2\right), \tag{3}$$

$$u\frac{\partial C}{\partial x}+v\frac{\partial C}{\partial y}=D_m\frac{\partial^2 C}{\partial y^2}-k_0(x)(C-C_\infty), \tag{4}$$

And the representing boundary conditions are

$$\left.\begin{array}{l} u(x,y)=U_w(x), v\left(x,y\right)=0, \\ -k\dfrac{\partial T}{\partial y}=h_1\left(T_w-T\right), -D_B\dfrac{\partial C}{\partial y}=h_2\left(C_w-C\right) \text{ at } y=0 \\ and \\ u=0,\ T=T_\infty\ ,\ C=C_\infty\ at\ y=\infty \end{array}\right\} \tag{5}$$

Where

$$\left.\begin{array}{l} \mu\left(T\right)=\mu*\left[a_1+b_1\left(1-\theta\right)\left(T_w-T_\infty\right)\right], B(x)=B_0\left(x+c\right)^{\frac{n-1}{2}}, \\ T_w\left(x\right)=T_\infty+T_0\left(x+c\right)^{\frac{1-n}{2}}, \mathrm{C}_w\left(x\right)=C_\infty+C_0\left(x+c\right)^{\frac{1-n}{2}} \end{array}\right\} \tag{6}$$

With the utilization of the following similarity transmutations [32], we change the governing equations as nonlinear ordinary differential equations.

$$\left.\begin{aligned}
&\zeta = y\sqrt{\frac{n+1}{2} b \frac{(x+c)^{n-1}}{\upsilon}}, u = b(x+c)^n \frac{df}{d\zeta}, k_0(x) = \left(x+c\right)^{n-1}, \\
&v = -\sqrt{\frac{n+1}{2}\upsilon b(x+c)^{n-1}}\left[\ \zeta \frac{df}{d\zeta}\ \left(\frac{n-1}{n+1}\right) + f(\zeta)\right], \\
&T = T_\infty + \left(T_w(x) - T_\infty\right)\theta\left(\zeta\right), C = C_\infty + \left(C_w(x) - C_\infty\right)\phi\left(\zeta\right)
\end{aligned}\right\} \tag{7}$$

By using (6) and (7), equations (2)-(4) changed as the below differential equations:

$$\left(a_1 + A\left(1-\theta\right)\right)\frac{d^3 f}{d\zeta^3} - \frac{2n}{n+1}\frac{d^2 f}{d\zeta^2} + f\frac{d^2 f}{d\zeta^2} - \frac{2}{n+1}M\frac{df}{d\zeta} - A\frac{d\theta}{d\zeta}\frac{d^2 f}{d\zeta^2} = 0 \tag{8}$$

$$\frac{d^2\theta}{d\zeta^2} + \Pr\left(f\frac{d\theta}{d\zeta} - \frac{1-n}{n+1}\frac{df}{d\zeta}\theta + Ec\left(\frac{d^2 f}{d\zeta^2}\right)^2\right) = 0 \tag{9}$$

$$\frac{d^2\phi}{d\zeta^2} + Sc\left(f\frac{d\theta}{d\zeta} - \frac{1-n}{n+1}\frac{df}{d\zeta}\phi - \frac{2}{n+1}Kr\phi\right) = 0 \tag{10}$$

And the corresponding boundary conditions changed as

$$\left.\begin{aligned}
&f(0) = \lambda\left(\frac{1-n}{n+1}\right), \left.\frac{df}{d\zeta}\right|_{\zeta=0} = 1, \\
&\left.\frac{d\theta}{d\zeta}\right|_{\zeta=0} = -\beta_1\left[1-\theta(0)\right], \left.\frac{d\phi}{d\zeta}\right|_{\zeta=0} = -\beta_2\left[1-\phi(0)\right], \\
&\left.\frac{df}{d\zeta}\right|_{\zeta=\infty} = 0, \theta(\infty) = 0, \phi(\infty) = 0
\end{aligned}\right\} \tag{11}$$

Where $A, M, \Pr, Ec, Sc, Kr$ are defined as

$$\left.\begin{aligned}
&A = b_1\left(T_w - T_\infty\right), M = \frac{\sigma B_0^2}{\rho b}, \Pr = \frac{\mu C_p}{k}, \\
&Ec = \frac{b^2\left(x+c\right)^{\frac{5n-1}{2}}}{C_p}, Sc = \frac{\upsilon}{D_m}, Kr = \frac{k_0}{b}
\end{aligned}\right\} \tag{12}$$

The essential physical measures of concern, the friction factor, the local Nusselt number and the Sherwood numbers are indicated as below:

$$\left.\begin{aligned} &C_f = 2\left(\frac{n+1}{2}\right)^{0.5} \left(\mathrm{Re}_x\right)^{-1/2} \left.\frac{d^2 f}{d\zeta^2}\right|_{\zeta=0}, \; Nu_x = -\left(\frac{n+1}{2}\right)^{0.5} \left(\mathrm{Re}_x\right)^{1/2} \left.\frac{d\theta}{d\zeta}\right|_{\zeta=0} \\ &\mathrm{Sh}_x = -\left(\frac{n+1}{2}\right)^{0.5} \left(\mathrm{Re}_x\right)^{1/2} \left.\frac{d\phi}{d\zeta}\right|_{\zeta=0} \end{aligned}\right\} \tag{13}$$

Where Re_x is the local Reynolds number characterized as $\mathrm{Re}_x = \dfrac{U_w(x)\left(x+c\right)}{\upsilon}$

3. Results and Discussion

The set of administering equations (7) - (9) with the boundary conditions (9) is settled with the guide of classical Runge-Kutta strategy based shooting technique. To analyze the three basic profiles (velocity, temperature, and concentration) through graphs for the impacts of different parameters, we utilize the following: $M = 2,\ a_1 = 1,\ n = 0.65$, $A = 0.5,\ Ec = 0.3,\ Sc = 1,\ Kr = 0.5,$ $\lambda = 0.3,\ \beta_1 = 0.2,\ \beta_2 = 0.2$. The friction factor, heat and mass transfer rates are explained through the tables.

More often than not, Lorentz force rises while moving electrically directed fluid particles influenced by the magnetic field parameter. So velocity diminishes and the other two (temperature and concentration) increase with the effect of M, as portrayed in Figs. 2-4. Fig. 5 explains that the Ec raises the temperature. With the increase in Ec, the heat transfer is laid in the fluid owing to friction forces which upgrade the temperature profile. From Figs. 6-8, it is clear that λ lessens all the three profiles. The reasons behind this may be the following: (a) generally, wall thickness opposes the flow. So velocity reduces with the rise in the wall thickness parameter (b) the reduction of temperature occurs because of less heat transfer from the denser areas to the flow than the more slender areas. Schmidt number lessens the thickness of the concentration boundary layer. As a consequence, concentration reduces with the increment in Sc which is displayed Fig. 9.

It is evident from the Fig. 10 that β_1 elevates the temperature. As β_1 is characterized as the proportion of the convection heat transfer to the conduction heat transfer, an increase in β_1 suggesting immense temperature at the sheet which helps to improve the denseness of the thermal boundary layer. Fig. 11 uncovers the fact that β_2 increases the concentration. The nature of Kr is to lessen the concentration which appears in Fig. 12. Viscosity variation parameter A, lessens the velocity, but shows the opposite behavior on the temperature and concentration profiles. This demonstrates the natural behavior of the viscosity (resists the flow as well as improve the denseness of the thermal boundary layer).

In Table 1, we exhibited the impact of previously mentioned parameters on the friction factor, the local Nusselt and Sherwood numbers in the form of values. It is clear that M, Ec, A lessen the rate of heat transfer as well as the rate of mass transfer. However, with the rise in the values of λ, Sc, β_2, Kr, mass transfer at the wall (Sherwood number) raises. Except Sc, β_2, Kr, all other parameters lessen the friction factor. It is noticed that the impact of β_1 and A on the mass transfer rate is negligible whereas λ and β_1 help in increasing the heat transfer rate. Table 2 exhibit the numerical validation of the results by comparing with the other techniques.

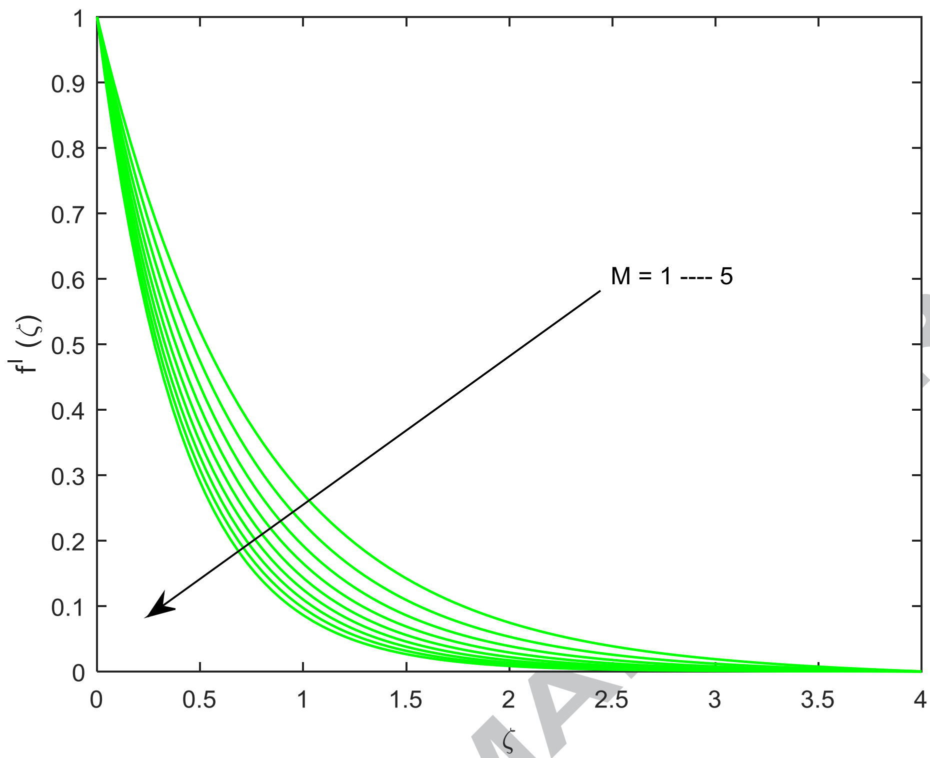

Fig. 2 Velocity profiles for different values of M

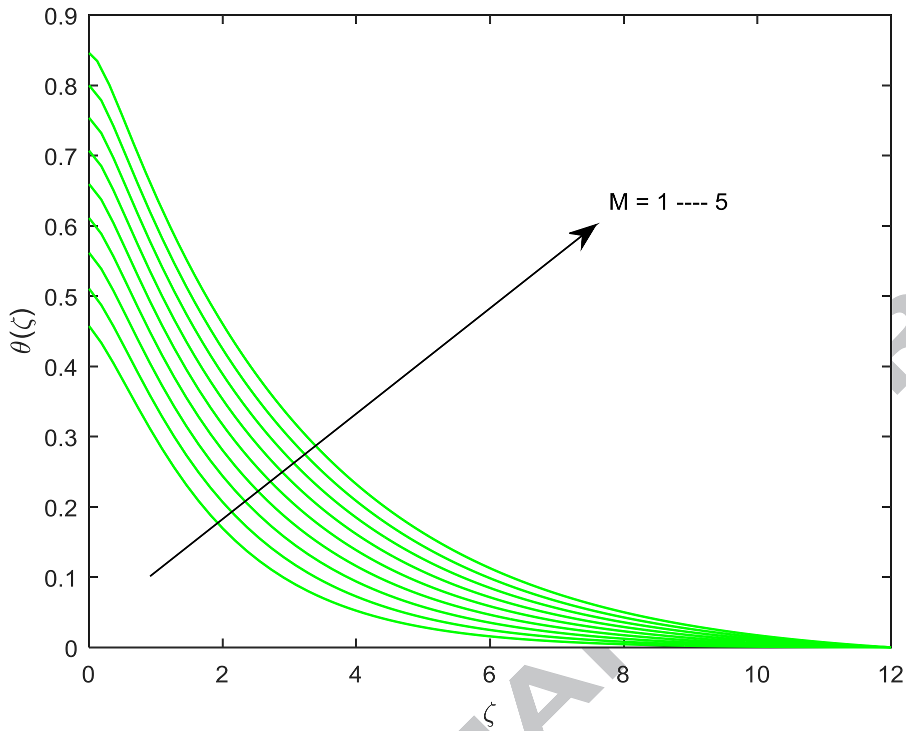

Fig. 3 Temperature profiles for different values of M

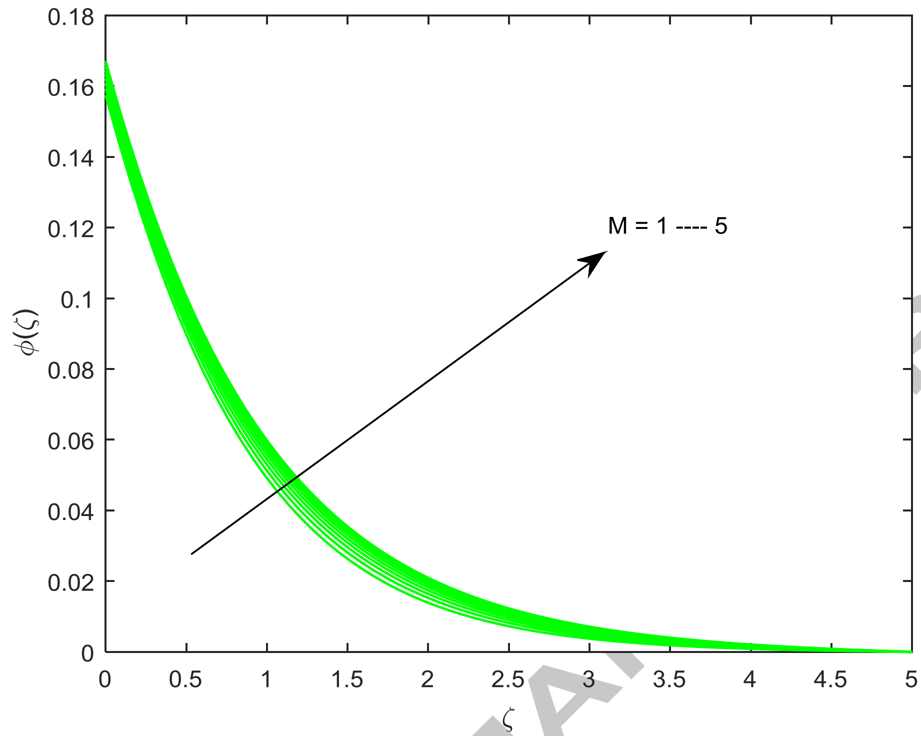

Fig. 4 Concentration profiles for different values of M

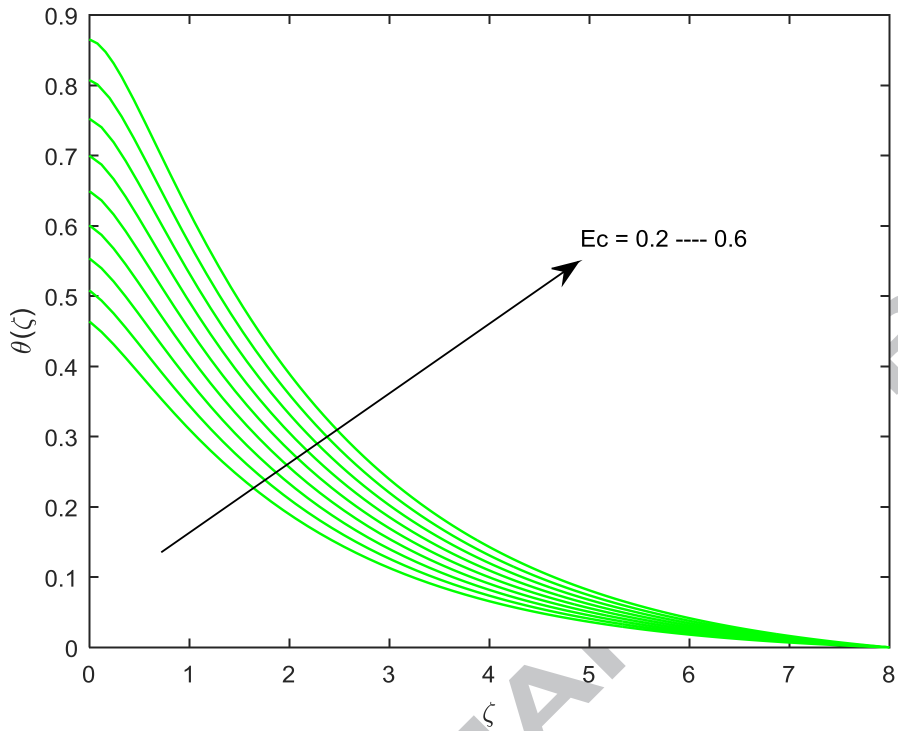

Fig. 5 Temperature profiles for different values of Ec

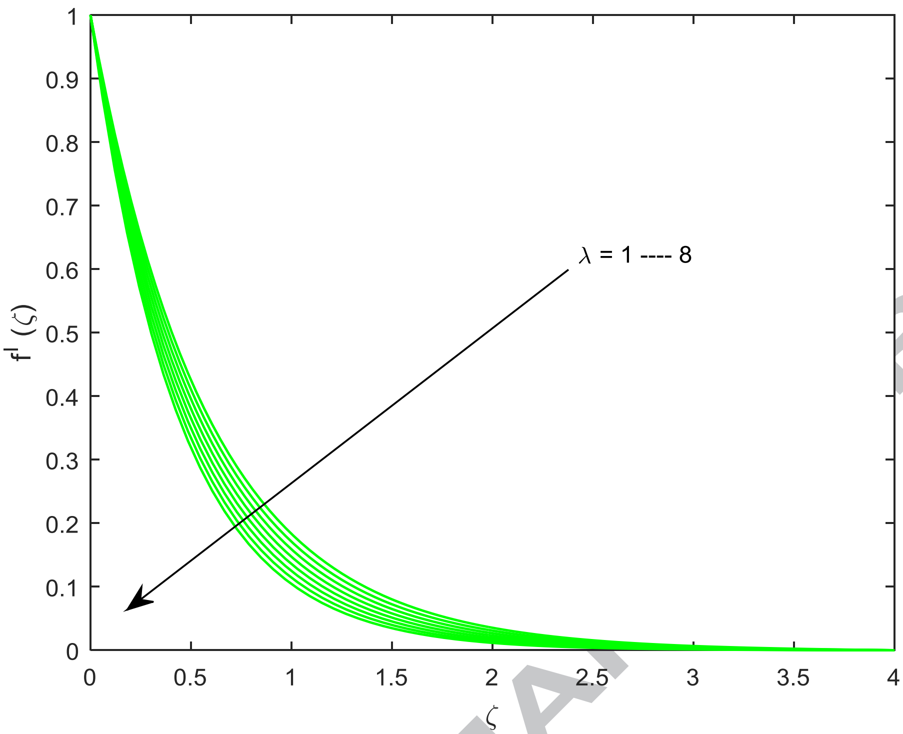

Fig. 6 Velocity profiles for different values of λ

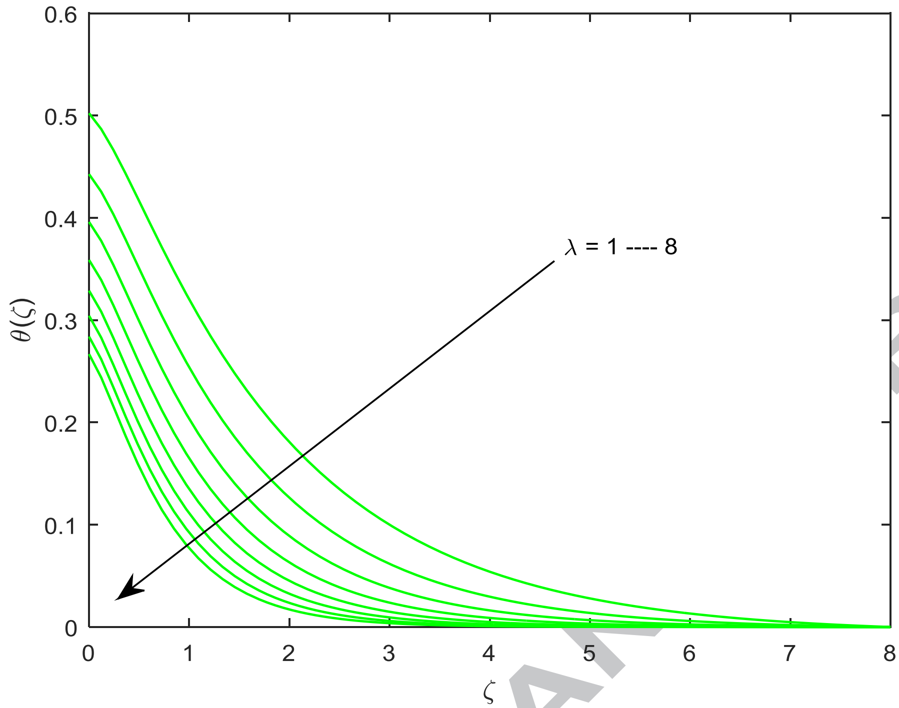

Fig. 7 Temperature profiles for different values of λ

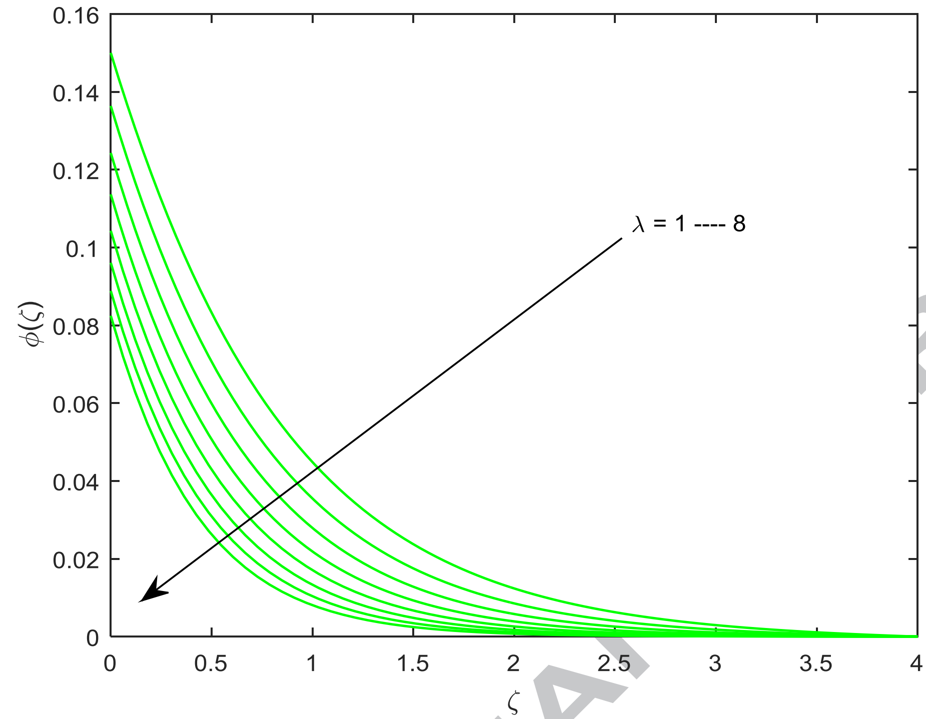

Fig. 8 Concentration profiles for different values of λ

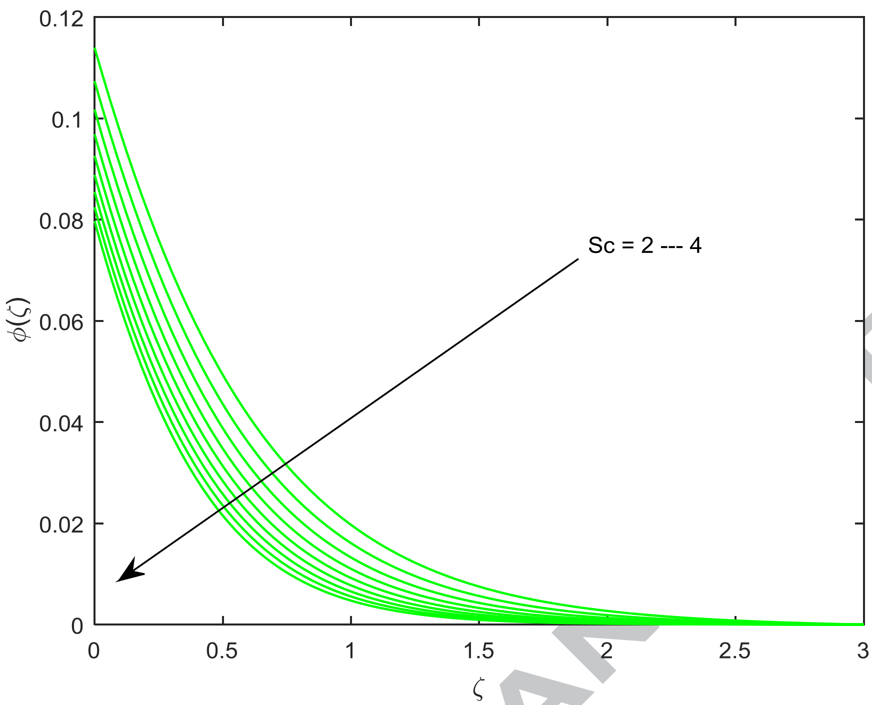

Fig. 9 Concentration profiles for different values of *Sc*

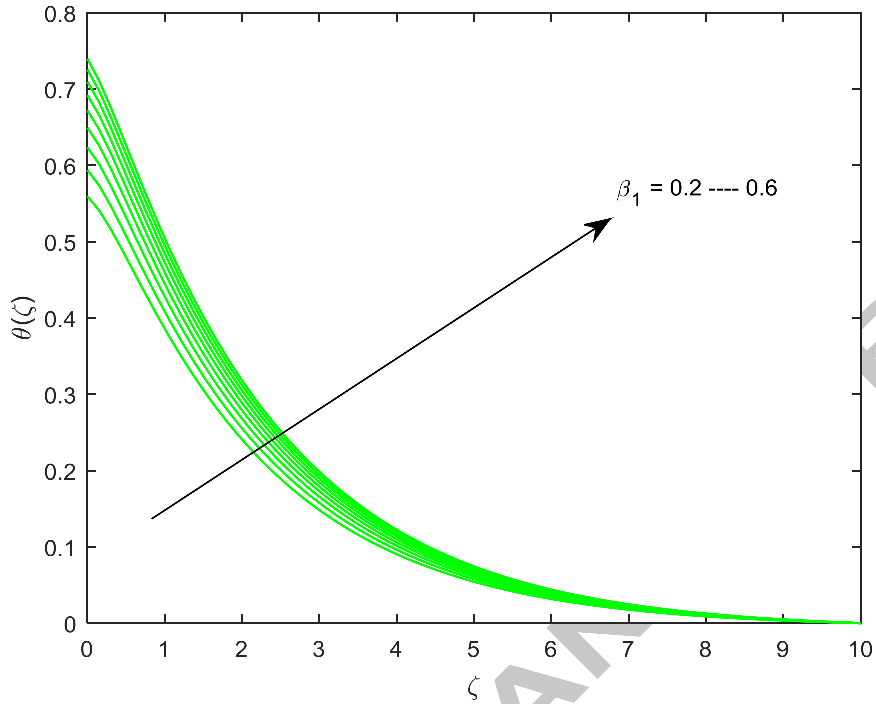

Fig. 10 Temperature profiles for different values of β_1

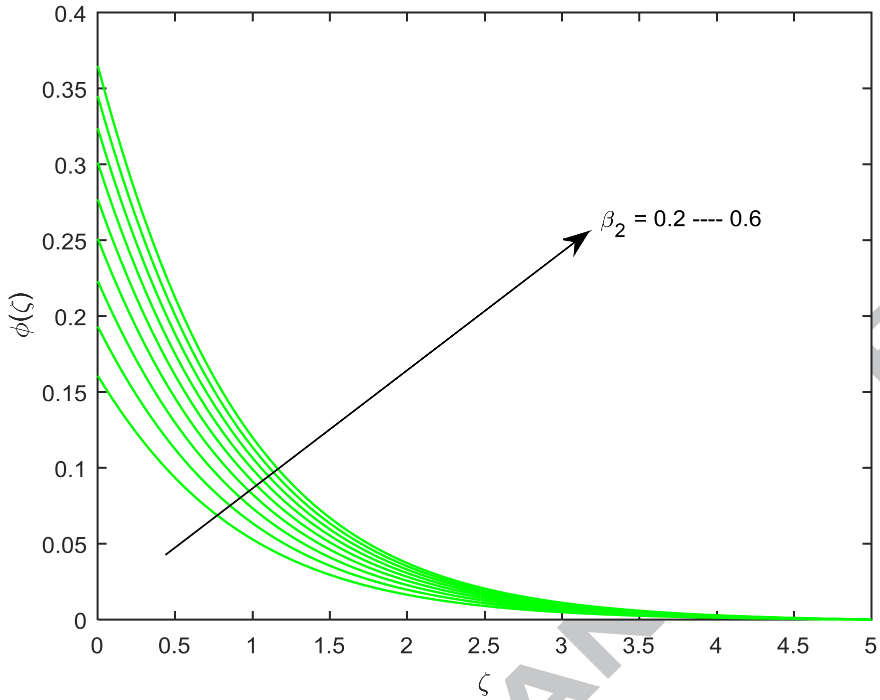

Fig. 11 Concentration profiles for different values of β_2

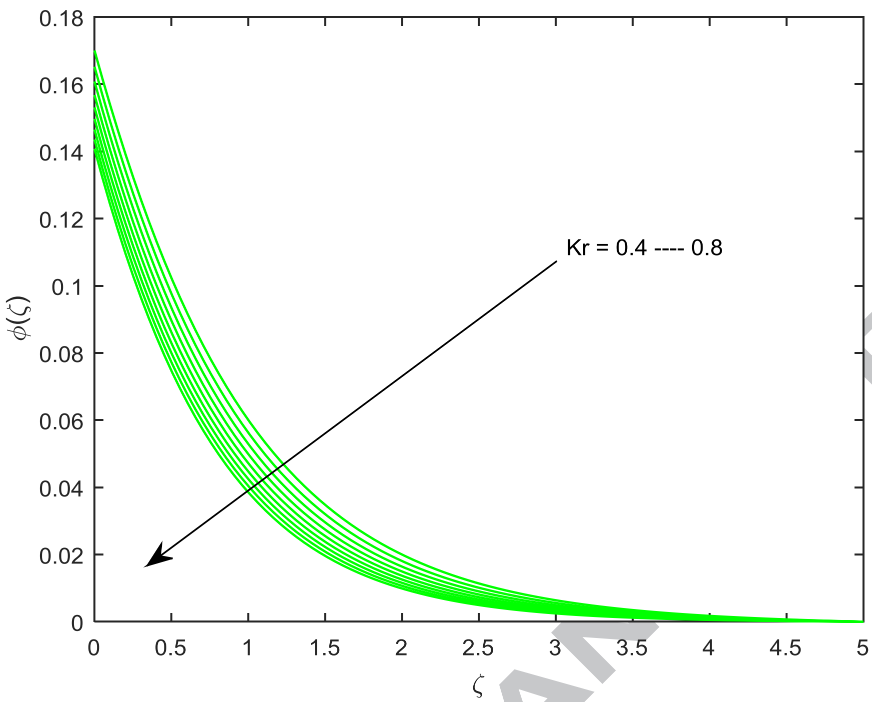

Fig. 12 Concentration profiles for different Kr

Table 1 The effect of different parameters on the friction factor, local Nusselt and the Sherwood numbers in terms of values

M	Ec	λ	Sc	β_1	β_2	Kr	A	$f''(0)$	$-\theta'(0)$	$-\phi'(0)$
1								-1.308178	0.115245	0.168546
2								-1.662102	0.100166	0.167888
3								-1.965126	0.086884	0.167393
	0.2							-1.648289	0.107210	0.167870
	0.3							-1.679902	0.089271	0.167814
	0.4							-1.715608	0.070135	0.167753
		1						-1.711883	0.107082	0.169993
		2						-1.786025	0.115823	0.172771
		3						-1.863899	0.123301	0.175137
			2					-1.649401	0.108530	0.177203
			3					-1.649401	0.108530	0.181474
			4					-1.649401	0.108530	0.184057
				0.2				-1.681797	0.088135	0.167811
				0.3				-1.707280	0.112911	0.167772
				0.4				-1.727150	0.131196	0.167741
					0.2			-1.670091	0.095216	0.167840
					0.3			-1.670091	0.095216	0.233025
					0.4			-1.670091	0.095216	0.289180
						0.2		-1.670091	0.095216	0.160787
						0.3		-1.670091	0.095216	0.163714
						0.4		-1.670091	0.095216	0.165992
							0.5	-1.889172	-0.007535	0.167478
							0.6	-1.900625	-0.008296	0.167467
							0.7	-1.913637	-0.009229	0.167454

Table 2 Validation of the numerical technique by comparing with the others for $-\theta'(0)$

M	RKS	$bvp4c$	$bvp5c$
1	0.115245	0.1152451342	0.1152451342
2	0.100166	0.1001668710	0.1001668711
3	0.086884	0.0868845644	0.0868845643
4	0.006452	0.0064522314	0.0064522314

4. Conclusions

The boundary layer flow across a slendering stretching sheet has gotten awesome consideration due to its inexhaustible pragmatic applications in nuclear reactor technology, acoustical components, chemical and manufacturing procedures. By keeping this in view, we analyzed the two-dimensional MHD fluid flow across a slendering stretching sheet within the sight of variable viscosity and viscous dissipation parameters. The principle discoveries are as per the following:

- M, Ec, β_1 and A are useful to enhance the temperature.
- λ improves both heat and mass transfer rates.
- Sc, β_2, Kr shows no impact on the rate of heat transfer.
- β_2 and A both enhance the concentration.
- The behavior of the velocity profile is quite opposite to that of concentration profile when they are affected by A.
- The effect of Sc and λ on concentration is similar.
- β_2 and A are not affecting the mass transfer rate.

Acknowledgment

The authors extend their appreciation to the Deanship of Scientific Research at King Saud University for funding this work through the research group project No RGP-080.

References

1. E.M.A. Elbashbeshy, Free convection flow with variable viscosity and thermal diffusivity along a vertical plate in the presence of the magnetic field, International Journal of Engineering Science 38 (2000) 207-213.

2. M.A. Hossain, K. Khanafer and K. Vafai, The effect of radiation on free convection flow of fluid with variable viscosity from a porous vertical plate, Int. J. Therm. Sci. 40 (2001) 115-124.
3. M.A. Seddeek, Effects of radiation and variable viscosity on a MHD free convection flow past a semi-infinite flat plate with an aligned magnetic field in the case of unsteady flow, International Journal of Heat and Mass Transfer 45 (2002) 931-935.
4. M. S. Abel, S.K. Khan and K.V. Prasad, Study of visco-elastic fluid flow and heat transfer over a stretching sheet with variable viscosity, International Journal of Non-Linear Mechanics 37 (2002) 81-88.
5. S. Mukhopadhyay, G.C. Layek and Sk.A. Samad, Study of MHD boundary layer flow over a heated stretching sheet with variable viscosity, International Journal of Heat and Mass Transfer 48 (2005) 4460-4466.
6. A. Hassanien, A.H. Essawy and N.M. Moursy, Variable viscosity and thermal conductivity effects on heat transfer by natural convection from a cone and a wedge in porous media, Arch. Mech., 55 (4) (2003) 345-355.
7. M.E. Ali, The effect of variable viscosity on mixed convection heat transfer along a vertical moving surface, International Journal of Thermal Sciences 45 (2006) 60-69.
8. A. Pantokratoras, The Falkner-Skan flow with constant wall temperature and variable viscosity, International Journal of Thermal Sciences 45 (2006) 378-389.
9. A.A. Afify, Effects of variable viscosity on non-Darcy MHD free convection along a non-isothermal vertical surface in a thermally stratified porous medium, Applied Mathematical Modelling 31 (2007) 1621-1634.

10. M.A. Seddeek, A.A. Darwish and M.S. Abdelmeguid, Effects of chemical reaction and variable viscosity on hydromagnetic mixed convection heat and mass transfer for Hiemenz flow through porous media with radiation, Communications in Nonlinear Science and Numerical Simulation 12 (2007) 195-213.
11. O.D. Makinde and A. Ogulu, The effect of thermal radiation on the heat and mass transfer flow of a variable viscosity fluid past a vertical porous plate permeated by a transverse magnetic field, Chem. Eng. Comm., 195 (2008) 1575-1584.
12. K.V. Prasad, D. Pal, V. Umesh and N.S. Prasanna Rao, The effect of variable viscosity on MHD viscoelastic fluid flow and heat transfer over a stretching sheet, Commun Nonlinear Sci Numer Simulat 15 (2010) 331-344.
13. O.D. Makinde, Second law analysis for variable viscosity hydromagnetic boundary layer flow with thermal radiation and Newtonian heating, Entropy 13 (2011) 1446-1464.
14. K. Vajravelu, K.V. Prasad and NG Chiu-On, The effect of variable viscosity on the flow and heat transfer of a viscous Ag-water and Cu-water nanofluids, Journal of Hydrodynamics 25 (1) (2013) 1-9.
15. S. Khamis, D.O. Makinde and Y. Nkansah-Gyekye, Unsteady flow of variable viscosity Cu-water and Al_2O_3-water nanofluids in a porous pipe with buoyancy force, International Journal of Numerical Methods for Heat & Fluid Flow 25 (7) (2015) 1638-1657.
16. W.A. Khan, O.D. Makinde and Z.H. Khan, Non-aligned MHD stagnation point flow of variable viscosity nanofluids past a stretching sheet with radiative heat, International Journal of Heat and Mass Transfer 96 (2016) 525-534.

17. O.D. Makinde and A. Aziz, MHD mixed convection from a vertical plate embedded in a porous medium with a convective boundary condition, International Journal of Thermal Sciences 49 (2010) 1813-1820.
18. O.D. Makinde and A. Aziz, Boundary layer flow of a nanofluid past a stretching sheet with a convective boundary condition, International Journal of Thermal Sciences 20 (2011) 1326-1332.
19. T. Hayat, S.A. Shehzad, A. Alsaedi and M.S. Alhothuali, Mixed convection stagnation point flow of Casson fluid with convective boundary conditions, Chin. Phys. Lett. 29(11) (2012)114704.
20. A. Alsaedi, M. Awais and T. Hayat, Effects of heat generation/absorption on stagnation point flow of nanofluid over a surface with convective boundary conditions, Commun Nonlinear Sci Numer Simulat 17 (2012) 4210-4223.
21. A. Noghrehabadi, R. Pourrajab and M. Ghalambaz, Flow and heat transfer of nanofluids over stretching sheet taking into account partial slip and thermal convective boundary conditions, Heat Mass Transfer 49 (2013) 1357-1366.
22. M. Qasim, Soret and Dufour effects on the flow of an Eyring-Powell fluid over a flat plate with convective boundary condition, Eur. Phys. J. Plus 129 (24) (2014) 1-7.
23. S. Nadeem, R. Mehmood and N.S. Akbar, Optimized analytical solution for oblique flow of a Casson-nano fluid with convective boundary conditions, International Journal of Thermal Sciences 78 (2014) 90-100.
24. M. Rahman, A.V. Rosca and I. Pop, Boundary layer flow of a nanofluid past a permeable exponentially shrinking surface with convective boundary condition using Buongiorno's

model, International Journal of Numerical Methods for Heat & Fluid Flow 25 (2) 2015 299-319.

25. G. Ibanez, Entropy generation in MHD porous channel with hydrodynamic slip and convective boundary conditions, International Journal of Heat and Mass Transfer 80 (2015) 274-280.
26. R. Kandasamy, C. Jeyabalan and K.K. Sivagnana Prabhu, Nanoparticle volume fraction with heat and mass transfer on MHD mixed convection flow in a nanofluid in the presence of thermo-diffusion under convective boundary condition, Appl Nanosci (2015) doi: 10.1007/s13204-015-0435-5.
27. M. Waqas, M. Farooq, M.I. Khan, A. Alsaedi, T. Hayat and T. Yasmeen, Magnetohydrodynamic (MHD) mixed convection flow of micropolar liquid due to nonlinear stretched sheet with convective condition, International Journal of Heat and Mass Transfer 102 (2016) 766-772.
28. K. Naganthran and R. Nazar, Stagnation – point flow of a nanofluid past a stretching/shrinking sheet with heat generation/absorption and convective boundary condition, 1784 (2016) 050004 doi: 10.1063/1.4966823.
29. T. Fang, J. Zhang and Y. Zhong, Boundary layer flow over a stretching sheet with variable thickness, Applied Mathematics and Computation 218 (2012) 7241-7252.
30. M.M. Khader and A.M. Megahed, Boundary layer flow due to a stretching sheet with a variable thickness and slip velocity, Journal of Applied Mechanics and Technical Physics 56 (2) (2015) 241-247.

31. S.P. Anjali Devi and M. Prakash, Temperature dependent viscosity and thermal conductivity effects on hydromagnetic flow over a slendering stretching sheet, Journal of Nigerian Mathematical Society 34 (2015) 318-330.
32. S.P. Anjali Devi and M. Prakash, Slip flow effects over hydromagnetic forced convective flow over a slendering stretching sheet, Journal of Applied Fluid Mechanics 9 (2) (2016) 683-692.
33. M. Jayachandra Babu and N. Sandeep, Three-dimensional MHD slip flow of nanofluids over a slendering stretching sheet with thermophoresis and Brownian motion effects, Advanced Powder Technology 27(5) (2016) 2039-2050.
34. M. Jayachandra Babu and N. Sandeep, MHD non-Newtonian fluid flow over a slendering stretching sheet in the presence of cross-diffusion effects, Alexandria Engineering Journal 55 (2016) 2193-2201.
35. M.Ali, Experimental free convection heat transfer from inclined square cylinders, Heat and Mass transfer, 52 (2016) 1-13, doi:10.1007/s00231-016-1881-7
36. M.E.Ali, N.Sandeep, Cattaneo-Christov model for radiative heat transfer of magnetohydrodynamic Casson-ferrofluid: a numerical study, Results in Physics, 7 (2017) 21-30.
37. N.Sandeep, Effect of aligned magnetic field on liquid thin film flow of magnetic-nanofluid embedded with graphene nanoparticles, Advanced Powder Technology, 28 (2017) 865–875.
38. M.Jayachandra Babu, N.Sandeep, UCM flow across a melting surface in the presence of double stratification and cross-diffusion effects, Journal of Molecular Liquids, 232 (2017) 27-35.

39. N. Sandeep, Ram Prakash Sharma, M. Ferdows, Enhanced heat transfer in unsteady magnetohydrodynamic nanofluid flow embedded with aluminum alloy nanoparticles, Journal of Molecular Liquids 234 (2017) 437–443.

40. P. Mohan Krishna, N. Sandeep, Ram Prakash Sharma, Computational analysis of plane and parabolic flow of MHD Carreau fluid with buoyancy and exponential heat source effects, European Physical Journal Plus, 132: 202, 2017.

Highlights

- Mathematical model of MHD flow across a slendering stretching surface.
- Variable viscosity and dissipation effects are incorporated in the model.
- Free convective heat transfer is evaluated.
- Wall thickness regulates the heat and mass transfer rate.